Emerging Microbes & Infections
2025, VOL. 14, 2482695 (18 pages)
https://doi.org/10.1080/22221751.2025.2482695

Evaluation of global distribution, genetic evolution, and mammalian infectivity and pathogenicity of H13 and H16 avian influenza viruses[1]

Xiang Li1 [a], Ao Li[a], Fengyi Qu[a], Yi Li[a], Fangyuan Chen[a], Xinru Lv[a], Qing An[a], Mengdan Fei[a], Hongyu Chen[a], Hongrui Liang[b], Xiaotian Zhang[b], Jinghao Li[b], Mingyuan Yu[b], Siyuan Qin[b], Linhong Xie[b], Shenglai Yin[c], Zheng Huang[c], Siyuan Yang[d], Heting Sun[b], Xiang Li2 [a] and Hongliang Chai [a]

[a]College of Wildlife and Protected Area, Northeast Forestry University, Harbin, People's Republic of China; [b]Biological Disaster Prevention and Control Center, National Forestry and Grassland Administration, Shenyang, People's Republic of China; [c]College of Life Sciences, Nanjing Normal University, Nanjing, People's Republic of China; [d]Department of Animal Science and Technology, Heilongjiang Vocational College for Nationalities, Harbin, People's Republic of China

ABSTRACT

H13 and H16 subtype avian influenza viruses (AIVs) typically infect *Charadriiformes*, are widely distributed throughout coastal regions worldwide, and pose a risk of spill-over to mammals. Systematic research on the epidemiology, transmission dynamics, and biological characteristics of these subtypes remains limited. To address this gap, we analyzed 20 years of wild bird influenza surveillance data from China integrated with global influenza database information to reconstruct the global spatiotemporal distribution, transmission dynamics and public health implications of H13 and H16. During influenza surveillance, 28 H13 and 19 H16 viruses were isolated. The phylogenetic trees for the H13 and H16 viruses revealed that both subtypes could be classified into three distinct groups. Viruses from H13 Group A, H13 Group C, and H16 Group C demonstrated frequent genetic exchanges and intercontinental transmission on a global scale. Mapping host migration revealed overlap between virus spread and host migration pathways. Our results suggest that host migration is a key driver of widespread distribution, cross-regional spread, and gene exchange for some H13 and H16 lineages. Virus isolates exhibit high genetic diversity with rich genotypic variation. Most isolates carry mammalian-adaptive mutations, such as the G228S mutation in the HA protein. H13 and H16 isolates of multiple genotypes infected mice without prior adaptation and exhibited varying tissue tropism. In summary, these findings indicate that host migration patterns are closely associated with the evolution of H13 and H16 AIVs. The potential risk of mammalian infection is highlighted, as viruses carrying mammalian-adaptive mutations may lead to new infection cases.

ARTICLE HISTORY Received 14 January 2025; Revised 25 February 2025; Accepted 17 March 2025

KEYWORDS AIV; H13; H16; phylogenetic; pathogenicity

Introduction

The influenza A virus (IAV) is divided into different subtypes according to the surface glycoprotein haemagglutinin (HA) and neuraminidase (NA) antigen types. To date, HA has been divided into 19 subtypes (H1-H19), and NA has been divided into 11 subtypes (N1-N11) [1, 2]. Birds are the natural hosts of IAV, so IAV is often referred to as avian influenza virus (AIV). Wild waterfowl are considered the natural hosts of AIV and can carry 17 HA and 9 NA subtypes [3]. IIn particular, the globally widespread Anseriformes and Charadriiformes are the wild birds with the highest AIV detection rates, serving a unique role in the preservation, reassortment, and cross-regional as well as cross-host transmission of AIV [4]. Migratory birds carrying AIV can spread the virus to other wild birds and poultry through secretions, excreta, and body pollution in feed and water across wintering grounds, breeding grounds, and migration stops; therefore, one potential transmission chain is the "wild birds–poultry–humans" chain, which threatens global public health security [5]. Pathogenic AIVs in chickens can be divided into highly pathogenic avian influenza virus (HPAIV) and low pathogenic avian influenza virus (LPAIV). The H13 and H16 viruses are LPAIVs [6].

In 1977, the AIV subtype H13 was first detected in the North American gull [7]; this subtype is currently found in North America, South America, Europe, Asia, Africa, and Oceania [8, 9]. The AIV subtype H16 was first identified in 1975 and is currently present in North America, South America, Europe, and Asia [10–12]. Studies have shown that H13 and H16 LPAIVs have experienced many

CONTACT Hongliang Chai hongliang_chai@hotmail.com; Xiang Li2 xiang_li1120@hotmail.com; Heting Sun xiaofengsht@163.com; Siyuan Yang yangsiyuan0451@126.com

[1] Supplemental data for this article can be accessed online at https://doi.org/10.1080/22221751.2025.2482695.

intercontinental gene flow events through the seasonal migration of some pelagic gull populations [13, 14]. For example, H13N2 viruses isolated from great black-backed gulls in Canada contain four gene fragments from European populations; this species has been confirmed to migrate from Newfoundland, Canada, to the United Kingdom, Spain, and Portugal [15]. In addition, some gulls, such as brown-headed gulls, can also be infected by and spread H5Nx HPAIVs [16], and the migration route of this species passes through multiple countries affected by the H5N1 HPAIV, including China, Bangladesh, India, Myanmar, Thailand, Cambodia, and Vietnam [17]. Long-distance migration and infection with different AIV subtypes may lead to the intercontinental transmission of AIV and genetic reorganization of AIV, with a risk of potential outbreaks [18–22].

In recent years, the range of host species for H5Nx HPAIVs during epidemic infection is rich, including wild waterfowl, such as *Charadriiformes*, *Anseriformes*, and *Gruiformes*, and numerous types of forest birds and raptors. In contrast, the range of wild bird host species for the H13 and H16 viruses is limited to mainly waterfowl species, especially various gulls, and overflow from these species to other types of hosts is difficult. However, unlike other wild birds, some gulls live in environments closely related to human activities such as fishing, grazing, and tourism; this pattern of close contact with humans may increase the risk of transmission. Many studies have shown that the H13 and H16 viruses have developed amino acid mutations that can increase the ability of the virus to bind to human receptors [13]. For example, the G228S mutation (H3numbering) in the HA gene was detected in both the H13 and H16 viruses. In addition, in the United States in 1984, H13N2 virus was detected in the pilot whale. These results indicate that H13 and H16 viruses can infect mammals, posing potential risks to public health and safety. However, systematic research on the epidemic distribution, transmission dynamics, and biological characteristics of these viruses remains insufficient. Identifying key host species among the diverse gull populations closely associated with virus transmission could provide crucial data to support prevention and control efforts.

Therefore, this study was conducted using the epidemiological surveillance data of wild bird AIVs in 28 provinces of China from 2003 to 2022 combined with H13 and H16 data in the global influenza database, including viral sequences, epidemiological information, and migration data. The objectives of this study were to assess global spatiotemporal distribution and dynamic propagation remodelling, elucidating the relationship between the complex migration patterns of birds and the intercontinental transmission of the H13 and H16 viruses and the influence of migratory behaviour on viral gene exchange, rematching and genetic diversity expansion and to assess the infectivity and pathogenicity of the H13 and H16 isolates detected in China using mice. The aim was to provide a scientific basis for assessing the public health risk of the virus and developing global prevention and control strategies.

Materials and methods

Samples and virus isolation

The samples in this study were primarily sourced from wild birds, including wild waterfowl, shorebirds, forest birds, and raptors. H13 and H16 subtype AIVs are primarily isolated from shorebirds such as plovers, sandpipers, and gulls. Before sampling, we first confirm the host type using binoculars. For AIV-positive samples of H13 and H16, we conducted host species-level identification using specific primers [23]. In cases where species-level identification was not feasible, we used the observed host, such as "shorebird," as a general reference for the host species. To avoid disturbing the birds' lives and destroying their habitats, the fresh feces of wild birds were collected in the morning; oropharyngeal and cloacal swabs were obtained from sentinel ducks or captured wild birds; and organs were collected from dead birds. The collected samples were stored in phosphate-buffered saline containing penicillin, streptomycin sulfate, and glycerol at pH 7.4. The virus was then collected and purified, the treated sample supernatant was inoculated into 10-day-old specific-pathogen-free chicken embryos, which were incubated in a 37°C fully automatic incubator for 72 h, after which the allantoic fluid was collected. The hemagglutination test was performed on allantoic fluid collected within 24–72 h of collection, and RT-PCR was performed on samples with positive hemagglutination test results [24–27].

Bayesian discrete phylogenetic analysis

cDNA from positive samples was amplified using PCR, and complete viral genome sequences were obtained via Sanger sequencing. The DNA sequences were viewed and assembled using EditSeq and SeqMan Pro in the DNAStar package. Multiple sequence alignments were performed using MAFFT [28] within the PhyloSuite [29] software. To perform a discrete phylogenetic analysis of global H13 and H16 viruses, HA gene sequences and sample information for H13 and H16 viruses were downloaded from the Global Initiative on Sharing All Influenza Data (GISAID) (https://platform.epicov.org/) and the National Center for Biotechnology Information (NCBI) (https://www.ncbi.nlm.nih.gov/genomes/FLU/) in October 2024. The data included sequences containing at least the HA gene and epidemiological information such as

collection date, location, and host species. Sequences with gene coverage less than 85% and incomplete collection dates were excluded. Both reference sequences and isolated sequences were included in subsequent analyzes. The best nucleotide substitution model, GTR + Empirical + G4, was identified using Modelfinder [30] in PhyloSuite on the basis of the Bayesian information criterion (BIC). Maximum likelihood (ML) trees were constructed using IQTREE with 1000 bootstrap replicates. The time signals for each dataset were examined via root-to-tip analysis in TempEst v1.5, and sequences with severe outlier patterns were removed. Bayesian phylogenetic dynamic analysis was performed on the dataset using BEAST v1.10.4 [31] with the Bayesian stochastic search variable selection (BSSVS) model. Two molecular clock models (uncorrelated log-normal relaxed clock model and strict clock model) were tested in combination with three tree priors (constant size, exponential growth, and Bayesian skyline). The best combination was determined via maximum likelihood estimation (MLE). The Markov chain Monte Carlo (MCMC) chains were set to 60–80 million iterations, with sampling every 10,000 steps. At least three independent runs were performed, and the results were combined. Tracer v1.7.1 was used to ensure that the effective sample size (ESS) was ≥200. The first 10% of burn-in values were discarded from each run, and the tree files from three runs were combined using Log Combiner v1.10.4. The combined tree files were annotated using TREE Annotator v1.10.4 to generate maximum clade credibility (MCC) trees [32–36]. Figtree v1.4.4 was used to visualize and annotate the MCC trees. To remove redundant sequences, we retained at least two virus sequences per month from each cluster in the MCC tree with identical hosts and isolation sources. The traits were divided into two categories: location and host. For location, H13 viruses were categorized into seven areas (Africa, Europe, Asia, China, North America, South America, and Oceania), and H16 viruses were categorized into six areas (Europe, Asia, China, North America, South America, and Oceania). Hosts were included if they had at least two sequences of the same species. If fewer than two sequences were available or the host was unknown, it was categorized as "other." Some H13 sequences included mixed hosts. Following the same methodology, we generated MCC trees of the HA genes of H13 and H16 viruses including location and host information for discrete phylogenetic analysis. Additionally, MCC trees for different groups were constructed using the same approach. Bayes factor (BF) values were calculated in SpreaD3 [37] using the log file from the BSSVS analysis. The results were included if BF values were ≥3 and posterior probabilities were ≥0.6.

Bayesian continuous phylogenetic analysis and phylogenetic incongruence analyzes

To analyze the continuous spatial diffusion of the three groups of H13 and H16 viruses, the sequences were processed with the method described in Section 2.2, with the traits changed to the latitude and longitude of the location. For China, Russia, the United States, Australia, Canada, and Kazakhstan, coordinates were specified to at least the provincial/state level. The MCC tree was generated and visualized using the "MCC tree with continuous traits" feature in SpreaD3. The results were opened in Firefox version 67.0 for annotation. Migratory bird data were obtained from publicly available datasets on the Movebank website [38]. We reviewed and summarized the migration routes of virus hosts with available data. Arrows were used to indicate migration routes, with thicker lines representing more host species along the route. A table listing the scientific and common names of all the species involved is included in the annex (Table S11). Reference sequences for the tanglegram were also downloaded from the two websites mentioned in Section 2.2. However, eight gene segments were needed, and sequences with less than 85% coverage were excluded. The best nucleotide substitution model was determined using Modelfinder in PhyloSuite on the basis of the BIC, and the ML tree was constructed with 1000 bootstrap replicates. The tanglegram was ordered as HA, PB2, PB1, PA, NP, M, NS, and NA, with only the N3 segment of the NA gene retained for H16 viruses. The basemap of the world map and the eight-segment tanglegram were generated using R packages, including ggplot2 [39], dplyr [40], ggtree [41], and ape [42]. The comprehensive visualization platform BioRender (https://BioRender.com) was used.

Mouse studies

Six-week-old BALB/c female mice (Vital River Laboratories, Beijing, China) were used to study the infectivity and pathogenicity of the H13 and H16 AIV subtypes in mammals. The mice were lightly anesthetized with CO_2, and a 50 µl volume of virus mixture with an EID_{50} content of 10^6 was seeded via nasal passages. Weight loss and mortality were monitored for 14 consecutive days. On the third day after inoculation, the brain, turbinate, lung, kidney, spleen, and rectum were collected for viral titration in 9- to 11-day-old SPF chicken embryos.

Ethics statement and experimental facility

All experiments involving live H13 and H16 AIVs and animals were carried out in the enhanced animal biosafety level 2+ (ABSL2+) facility at the College of

Wildlife and Protected Area, Northeast Forestry University, Harbin, China. All animal experiments were conducted in strict accordance with the recommendations of the Guide for the Care and Use of Laboratory Animals of the Ministry of Science and Technology of China. The animal study protocols were authorized the Committee on the Ethics of Animal Experiments of the NEFU.

Results

Active surveillance of AIVs in wild birds in China

Between 2003 and 2022, the active surveillance of wild bird AIVs included 28 provincial administrative regions in China, including Hubei, Hunan, Jiangxi, Anhui, Jiangsu, Shanghai, Heilongjiang, Hebei, Xinjiang, Shaanxi, Dandong, Fujian and Xizang. A total of 214,400 fecal samples from wild birds (mainly wild waterfowl), pharyngeal and anal swabs, and organ samples from dead birds were collected (Figure 1). A total of 28 H13 and 19 H16 viruses were isolated, among which 5 H16 viruses did not have complete sequences. The fully sequenced viruses included H13N6 ($n = 19$), H13N2 ($n = 5$), H13N8 ($n = 4$), H16N3 ($n = 13$), and H16N2 ($n = 1$), with the primary hosts belonging to the order *Charadriiformes* (Figure 1, Tables 1 and 2).

Bayesian discrete phylogenetic analysis

The phylogenetic tree (Figure 2(A)) shows that the HA gene segment in H13 virus subtypes can be categorized into three genetic groups (Groups A, B and C), with 28 isolates clustered in Groups A and C. The most recent

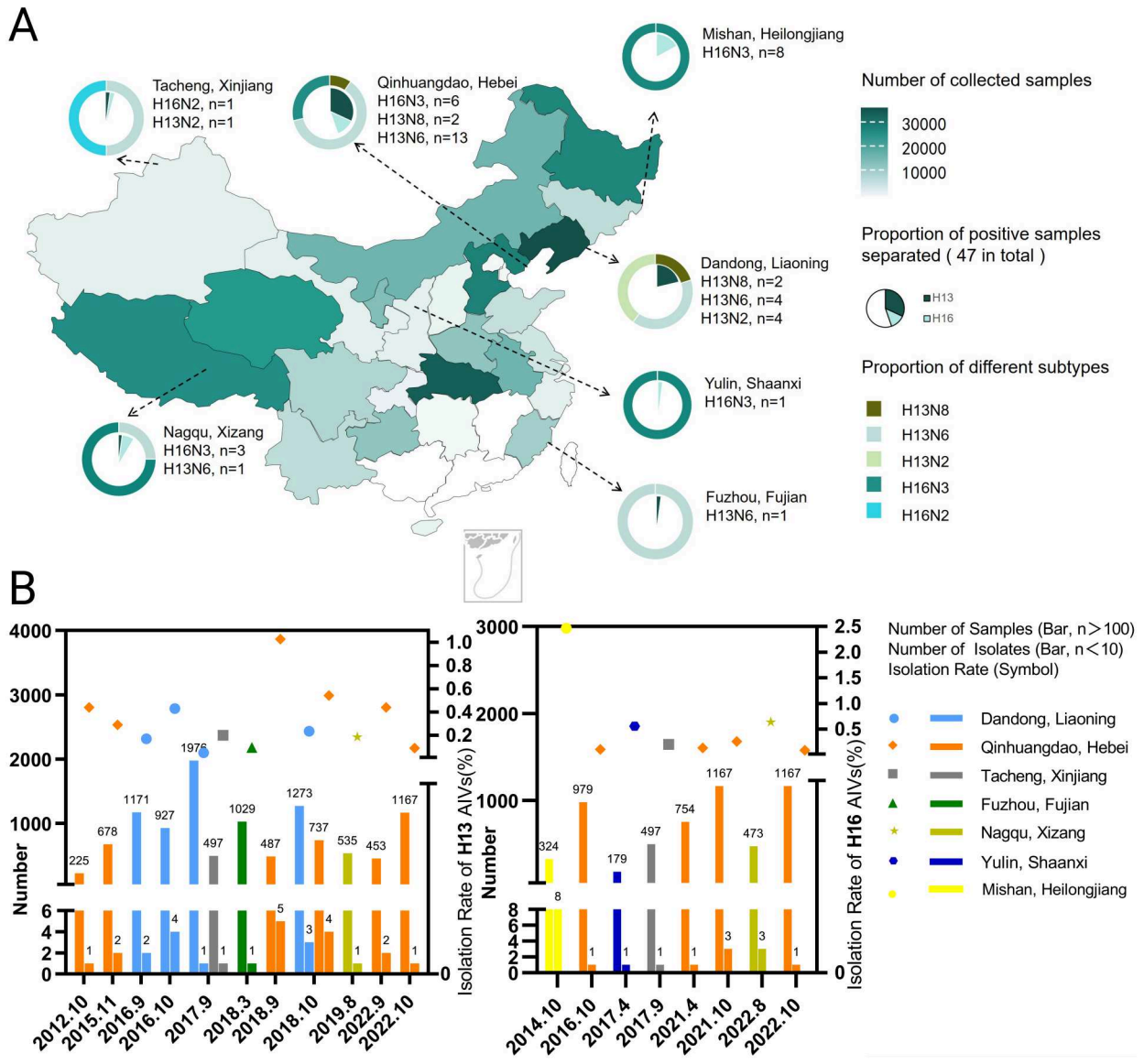

Figure 1. (A) Sampling of 28 provincial administrative regions in China and the provincial origin of isolates from each subtype of H13 and H16 avian influenza viruses in China between 2003 and 2022. (B) The sampling quantities, the number of positive samples, and the isolation rates for H13 and H16 AIVs are presented. The sampling quantities and the number of positive samples are displayed on the left *Y*-axis, while the isolation rates are shown on the right *Y*-axis.

Table 1. Information of the 28 H13 subtype AIVs isolated in wild birds in China.

No.	Isolates	Abbreviation	Sampling date	Sampling site (city, province)	Species	Sample type	Genotype	GISAID isolate Id
1	A/common black-headed gull/QHD/440-184/2012(H13N8)	G184	October, 2012	Qinhuangdao, Hebei	Black-headed gull (*Chroicocephalus ridibundus*)	Feces	G1	19645814
2	A/shorebird/Hebei/Qinhuangdao4581/2015(H13N8)	G4581	November, 2015	Qinhuangdao, Hebei	Shorebird	Feces	G2	19646685
3	A/shorebird/Hebei/Qinhuangdao3802/2015(H13N6)	G3802	November, 2015	Qinhuangdao, Hebei	Shorebird	Feces	G3	19646686
4	A/shorebird/Liaoning/Dandong478/2016(H13N8)	D478	September, 2016	Dandong, Liaoning	Shorebird	Feces	G4	19646687
5	A/shorebird/Liaoning/Dandong616/2016(H13N8)	D616	September, 2016	Dandong, Liaoning	Shorebird	Feces	G5	19646688
6	A/shorebird/Liaoning/Dandong538/2016(H13N2)	D538	October, 2016	Dandong, Liaoning	Shorebird	Feces	G6	19646689
7	A/glaucous gull/Liaoning/Dandong628/2016(H13N2)	D628	October, 2016	Dandong, Liaoning	Glaucous gull (*Larus hyperboreus*)	Feces	G7	19646690
8	A/shorebird/Liaoning/Dandong679/2016(H13N2)	D679	October, 2016	Dandong, Liaoning	Shorebird	Feces	G7	19646691
9	A/shorebird/Liaoning/Dandong457/2016(H13N2)	D457	October, 2016	Dandong, Liaoning	Shorebird	Feces	G7	19646692
10	A/shorebird/Liaoning/Dandong81/2017(H13N6)	D81	September, 2017	Dandong, Liaoning	Shorebird	Feces	G8	19646693
11	A/ kelp gull/Xinjiang/XJ126/2017(H13N2)	XJ126	September, 2017	Tacheng, Xinjiang	Kelp gull (*Larus dominicanus*)	Feces	G9	19646719
12	A/shorebird/Fujian/F541/2018(H13N6)	F541	March, 2018	Fuzhou, Fujian	Shorebird	Feces	G10	19646694
13	A/black-tailed gull/Hebei/Qinhuangdao477/2018(H13N6)	G477	September, 2018	Qinhuangdao, Hebei	Black-tailed gull (*Larus crassirostris*)	Feces	G10	19646724
14	A/shorebird/Liaoning/Dandong2008/2018(H13N6)	D2008	October, 2018	Dandong, Liaoning	Shorebird	Feces	G11	19646695
15	A/shorebird/Liaoning/Dandong2014/2018(H13N6)	D2014	October, 2018	Dandong, Liaoning	Shorebird	Feces	G11	19646696
16	A/shorebird/Liaoning/Dandong2146/2018(H13N6)	D2146	October, 2018	Dandong, Liaoning	Shorebird	Feces	G11	19646697
17	A/glaucous gull/Hebei/Qinhuangdao87/2018(H13N6)	G87	September, 2018	Qinhuangdao, Hebei	Glaucous gull (*Larus hyperboreus*)	Feces	G12	19646698
18	A/shorebird/Hebei/Qinhuangdao89/2018(H13N6)	G89	September, 2018	Qinhuangdao, Hebei	Shorebird	Feces	G12	19646699
19	A/shorebird/Hebei/Qinhuangdao181/2018(H13N6)	G181	September, 2018	Qinhuangdao, Hebei	Shorebird	Feces	G12	19646700
20	A/black-tialed-gull/Hebei/Qinhuangdao509/2018(H13N6)	G509	October, 2018	Qinhuangdao, Hebei	Black-tailed gull (*Larus crassirostris*)	Feces	G12	19646720
21	A/black-tailed-gull/Hebei/Qinhuangdao571/2018(H13N6)	G571	October, 2018	Qinhuangdao, Hebei	Black-tailed gull (*Larus crassirostris*)	Feces	G12	19646721
22	A/shorebird/Hebei/Qinhuangdao1106/2018(H13N6)	G1106	October, 2018	Qinhuangdao, Hebei	Shorebird	Feces	G12	19646701
23	A/brown-headed gull/Tibet/XZ529/2019(H13N6)	XZ529	August, 2019	Nagqu, Xizang	Brown-headed gull (*Chroicocephalus brunnicephalus*)	Feces	G12	19646725
24	A/black-tailed gull/Hebei/Qinhuangdao126/2018(H13N6)	G126	September, 2018	Qinhuangdao, Hebei	black-tailed gull (*Larus crassirostris*)	Feces	G13	19646722
25	A/black-tialed-gull/Hebei/Qinhuangdao384/2018(H13N6)	G384	October, 2018	Qinhuangdao, Hebei	Black-tailed gull (*Larus crassirostris*)	Feces	G14	19646723
26	A/black-headed-gull/Hebei/Qinhuangdao1606/2021(H13N6)	G1606	September, 2021	Qinhuangdao, Hebei	Black-headed gull (*Chroicocephalus ridibundus*)	Feces	G15	19646702

(*Continued*)

Table 1. Continued.

No.	Isolates	Abbreviation	Sampling date	Sampling site (city, province)	Species	Sample type	Genotype	GISAID isolate Id
27	A/black-headed-gull/Hebei/Qinhuangdao1501/2021(H13N6)	G1501	September, 2021	Qinhuangdao, Hebei	Black-headed gull (*Chroicocephalus ridibundus*)	Feces	G16	19646703
28	A/shorebird/Hebei/Qinhuangdao1791/2021(H13N6)	G1791	October, 2021	Qinhuangdao, Hebei	Shorebird	Feces	G17	19646704

common ancestor of the HA gene is estimated to date back to 1928. The most recent common ancestors of Groups A, B, and C are estimated to date back to 1974, 1975, and 1976, respectively. The viruses in Group A are from America, Europe, and Asia; the viruses in Group B are from America and Europe; and the viruses in Group C are from Africa, America, Europe, Asia, and Oceania. The Bayesian lineage dynamics analysis revealed 11 migration paths within the spatial diffusion of H13 viruses (Figure 3(A), Table S1). The main ancestor of H13 hosts is *Charadriiformes*; a small number of the hosts of Groups A and C (including 19 and 9 isolates in this study) are aquatic poultry, ducks, and other birds, and a small number of hosts of Group B are terrestrial poultry such as turkeys, mammals such as whales, and others. H13 viruses have 35 transmission routes for host spread (Figure 3(C), Table S2).

The phylogenetic tree (Figure 2(B)) revealed that the HA gene segment in the H16 virus can be characterized into three genetic groups (Groups A to C), with 14 isolates clustered in Groups A and C. The most recent common ancestor of the HA gene dates back to 1936. The most common ancestors for Groups A, B, and C are estimated to date back to 1979, 1971, and 1969, respectively. The viruses in Group A are from Europe and Asia; those in Group B are from North America; and those in Group C are from

Table 2. Information of the 14 H16 subtype AIVs isolated in wild birds in China.

No.	Isolates	Abbreviation	Sampling date	Sampling site (City, Province)	Species	Sample Type	Genotype	GISAID Isolate Id
1	A/Anatidae/Heilongjiang/M1/2014(H16N3)	M1	October, 2014	Mishan, Heilongjiang	Anatidae	Feces	G1	19646705
2	A/Anatidae/Heilongjiang/M7/2014(H16N3)	M7	October, 2014	Mishan, Heilongjiang	Anatidae	Feces	G1	19646706
3	A/Anatidae/Heilongjiang/M46/2014(H16N3)	M46	October, 2014	Mishan, Heilongjiang	Anatidae	Feces	G1	19646707
4	A/shorebird/Hebei/Qinhuangdao547/2016(H16N3)	G547	October, 2016	Qinhuangdao, Hebei	Shorebird	Feces	G2	19646708
5	A/black-headed gull/Shaanxi/e156/2017(H16N3)	E156	April, 2017	Yulin, Shaanxi	Black-headed gull (*Chroicocephalus ridibundus*)	Feces	G3	19646709
6	A/shorebird/Xinjiang/XJ56/2017(H16N2)	XJ56	September, 2017	Tacheng, Xinjiang	Shorebird	Feces	G4	19646710
7	A/black-headed-gull/Hebei/Qinhuangdao1356/2021(H16N3)	G1356	October, 2021	Qinhuangdao, Hebei	Black-headed gull (*Chroicocephalus ridibundus*)	Feces	G5	19646711
8	A/black-headed-gull/Hebei/Qinhuangdao1446/2021(H16N3)	G1446	October, 2021	Qinhuangdao, Hebei	Black-headed gull (*Chroicocephalus ridibundus*)	Feces	G5	19646712
9	A/black-headed-gull/Hebei/Qinhuangdao1286/2021(H16N3)	G1286	October, 2021	Qinhuangdao, Hebei	Black-headed gull (*Chroicocephalus ridibundus*)	Feces	G6	19646713
10	A/shorebird/Hebei/Qinhuangdao308/2021(H16N3)	G308	April, 2021	Qinhuangdao, Hebei	Shorebird	Feces	G7	19646714
11	A/shorebird/Tibet/XZ2636/2022(H16N3)	XZ2636	August, 2022	Nagqu, Xizang	Shorebird	Feces	G8	19646715
12	A/shorebird/Tibet/XZ2646/2022(H16N3)	XZ2646	August, 2022	Nagqu, Xizang	Shorebird	Feces	G8	19646716
13	A/brown-headed gull/Tibet/XZ2406/2022(H16N3)	XZ2406	August, 2022	Nagqu, Xizang	Brown-headed gull (*Chroicocephalus brunnicephalus*)	Feces	G8	19646726
14	A/shorebird/Hebei/Qinhuangdao1086/2022(H16N3)	G1086	October, 2022	Qinhuangdao, Hebei	Shorebird	Feces	G9	19646717

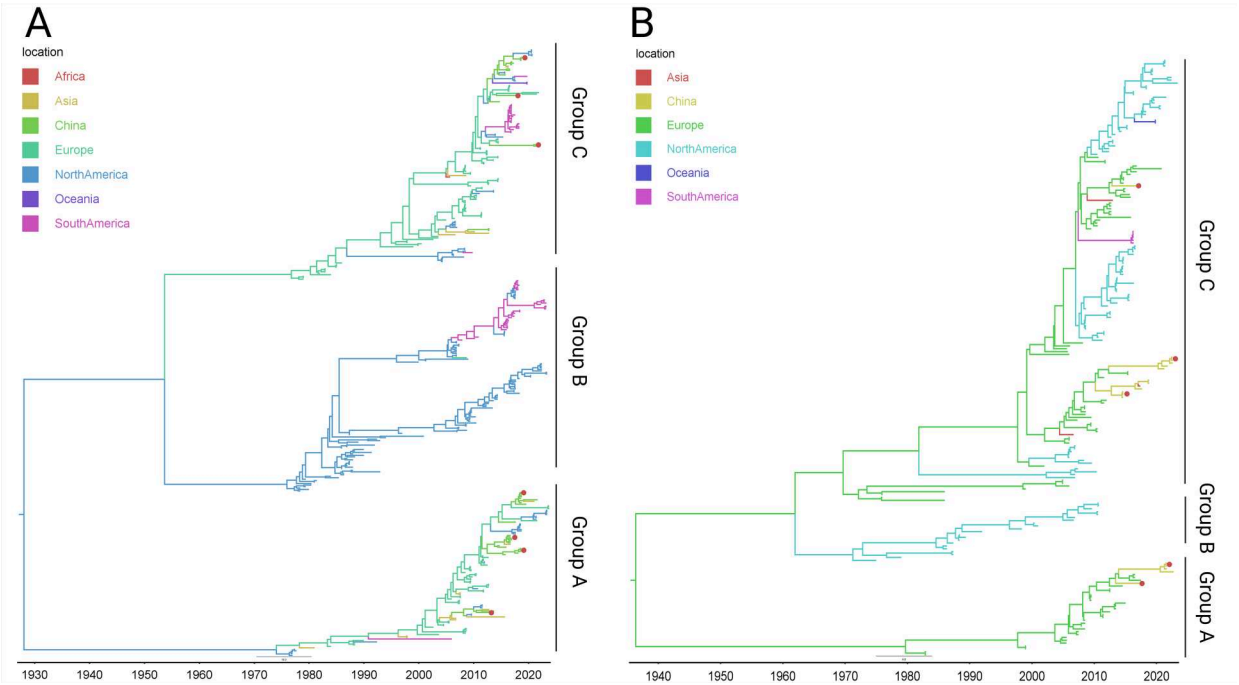

Figure 2. (A) MCC tree of the H13 gene of the H13 LPAIV 410 viruses, including 28 isolates in this study and 382 H13 reference viruses downloaded from the database. The horizontal axis is the time axis, and the red dotted region is the location of the 28 isolates in this study. (B) MCC tree of the H16 gene of H16 LPAIV 209 viruses, including 14 isolates from this study and 195 H16 reference viruses downloaded from the database. The horizontal axis is the time axis, and the red dotted region is the location of the 14 isolates in this study.

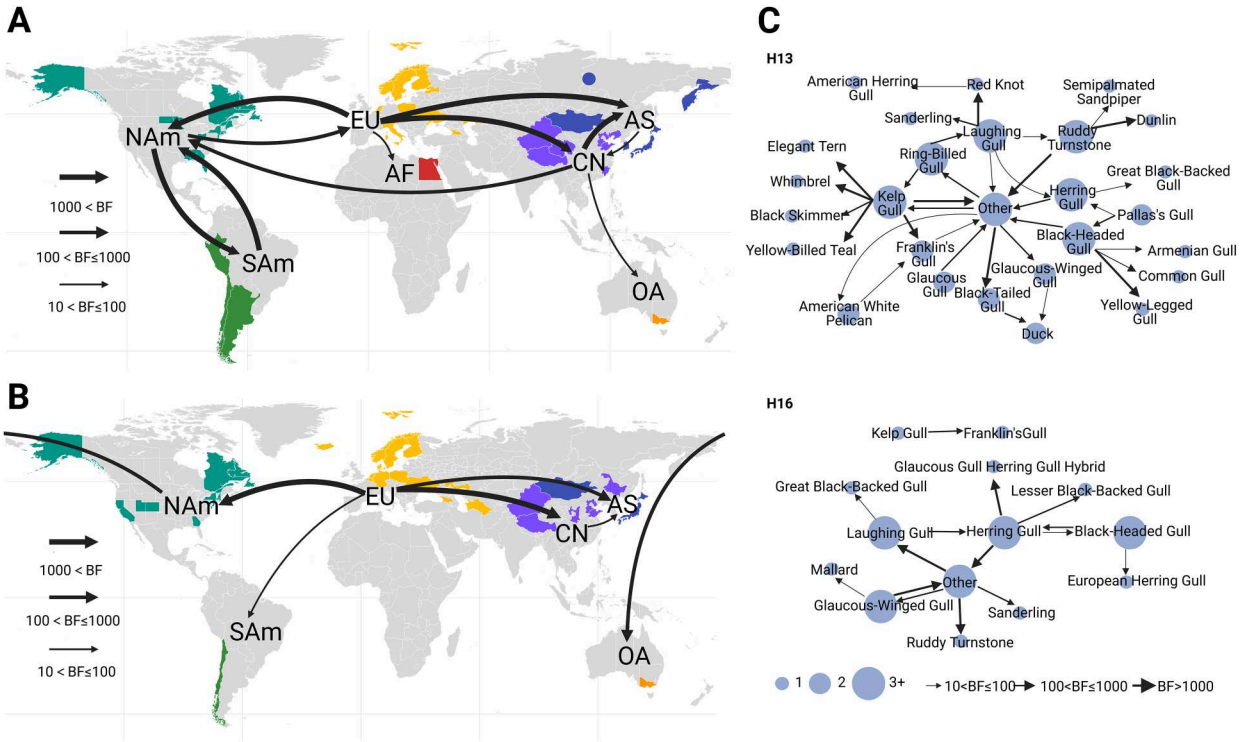

Figure 3. (A) Spatial diffusion of the H13 gene segment of global H13 avian influenza viruses. AF, Africa; OA, Oceania, AS, Asia; EU, Europe; NAm, North America; A; SAm, South America; CN, China. BF value of spatial diffusion: Europe to Asia (BF > 1000), Europe to China (BF > 1000), Europe to North America (BF > 1000), China to Asia (BF > 1000), South America to North America (BF > 1000), North America to South America (BF > 1000), China to North America (100 < BF ≤ 1000), North America to Europe (100 <BF ≤ 1000), Asia to China (10 < BF ≤ 100), China to Oceania (10 < BF ≤ 100), and Europe to Africa (10 < BF ≤ 100). The blue circles represent sequences from the Siberian region. (B) Spatial diffusion of the H16 gene segment of the global H16 virus. OA, Oceania; CN, China; AS, Asia; EU, Europe; NAm, North America; SAm, South America. BF value of spatial diffusion: Europe to China (BF > 1000), Europe to North America (BF > 1000), North America to Oceania (100 < BF ≤ 1000), Europe to Asia (100 < BF 1000), Europe to South America (10 <BF ≤ 100), and China to Asia (10 < BF ≤ 100). The blue circles represent sequences from the Siberian region. (C) The size of the blue circle represents the number of times involved in propagation.

Oceania, America, Europe, and Asia. Bayesian lineage dynamics analysis revealed six migration paths in the spatial diffusion of H16 viruses (Figure 3(B), Table S3). The main hosts of the H16 viruses are *Charadriiformes*. A small number of Group A hosts (including 5 isolates in this study) are classified as wild ducks, aquatic poultry, the environment, and others; a small number of the Group B hosts are classified as others; and the Group C hosts (including 9 isolates in this study) are all *Charadriiformes*. H16 viruses have 15 transmission routes for host spread (Figure 3(C), Table S4).

Phylogenetic analysis of different subgroups of H13 and H16

H13 AIVs

Continuous spatial diffusion analyzes of global H13 viruses were conducted based on the three branches identified by the HA gene MCC tree. Host information was analyzed using the discrete phylogenetic method. The characteristics of each branch are described below.

Group A is primarily distributed across Europe, the Americas, and Asia (Figure 4(A)). In China, isolates were found in both coastal and inland provinces, including Fujian, Hebei, Shandong, Liaoning, and Xizang. Geographic transmission analysis revealed that the spread of H13 Group A viruses involves six global migratory paths: Pacific America, Mississippi America, Atlantic America, East Atlantic, Central Asia, and East Asia-Australasia. The earliest detected isolates of Group A can be traced to Maryland, USA, in 1977. The geographical transmission centres of this branch are mainly in Europe and Central Asia, with early isolates found in Central Asia, Japan, and the east coast of the United States. Before 2005, the virus spread from the east coast of the United States to Central Asia and then further to Europe, the Americas, Siberia, and Asia. From 2005–2010, the virus spread from Europe to neighbouring regions, Central Asia, Mongolia, and the United States; the viruses in Central Asia spread to East Asia and Europe, and the viruses in Japan spread to the United States. Between 2010 and 2015, the viruses from Japan spread to China and the Kamchatka Peninsula in Russia before spreading back to Japan. The viruses in Europe spread to neighbouring regions, whereas viruses spread mutually between Central Asia and the United States. After 2015, the virus from the Bohai Bay region of China spread to the surrounding areas, Europe, Alaska (USA), and the Kamchatka Peninsula (Russia). The viruses in Central Asia spread to Europe, the United States, and China. Migratory data were available for the black-headed gull, dunlin, Eurasian curlew, glaucous gull, herring gull, red knot, mallard, ring-billed gull, ruddy turnstone, sanderling, and yellow-legged gull. Phylogeographic analysis of H13 Group A hosts revealed that major contributors to viral spread include the glaucous-winged gull, herring gull, and black-headed gull (Figure 4(G), Table S5).

Group B is primarily distributed in North America (the United States and Canada), South America (Chile and Peru), and Europe (Finland) (Figure 4(B)). Transmission of Group B viruses predominantly follows a north–south trajectory. None of the isolates analyzed in this study clustered within Group B. The geographical spread of H13 Group B viruses involves three global migratory paths: the Mississippi, Atlantic Americas, and Pacific Americas. The earliest record of a Group B virus traces to a 1978 isolate from Maryland, USA. Before 2010, viruses spread from the eastern United States to neighbouring regions, South America, and Europe. From 2010–2020, viruses expanded from South America to Alaska and Minnesota in the United States. Migratory information was available for the American herring gull, black skimmer, black-legged kittiwake, dunlin, herring gull, knot, red knot, mallard, ring-billed gull, ruddy turnstone, sanderling, semipalmated sandpiper, whimbrel, and yellow-legged gull. Phylogeographic analysis of H13 Group B hosts revealed that the major contributors to viral spread include the herring gull, laughing gull, and kelp gull (Figure 4(G), Table S5).

Group C is distributed across Europe, Asia, the Americas, Africa, and Oceania (Figure 4(C)). In North America, viruses are concentrated in Alaska and Minnesota, while South America has a significant number of viruses in Chile. The Eurasian region spans eight countries. In China, viruses are found in coastal and inland regions, including Xinjiang, Qinghai, Hebei, Shandong, and Liaoning. The spread of Group C viruses involves five major global migratory paths: the Mississippi, Black Sea-Mediterranean, Central Asian, and East Asian-Australasian. The earliest known Group C virus was isolated in Astrakhan, Russia, in 1979. The geographic spread of the isolates indicates that before 2005, the virus primarily spread from Central Asia to Europe and the east coast of the United States. From 2005–2010, the viruses spread from the central United States to Alaska and South America and from Europe and Central Asia to East Asia and Mongolia. Between 2010 and 2015, the viruses spread from Europe and Central Asia to the eastern United States, Alaska, and China, whereas the viruses in the United States spread to Europe, Central Asia, and South America. From 2015–2020, the viruses in Bohai Bay in China spread to Kamchatka, Russia, and Alaska, whereas those in Central Asia spread to Australia. The viruses in Europe spread to Mongolia, the United States, and Bohai Bay in China, whereas those in the central United States spread to South America. Migratory information was available for the American oystercatcher, black-headed gull, black

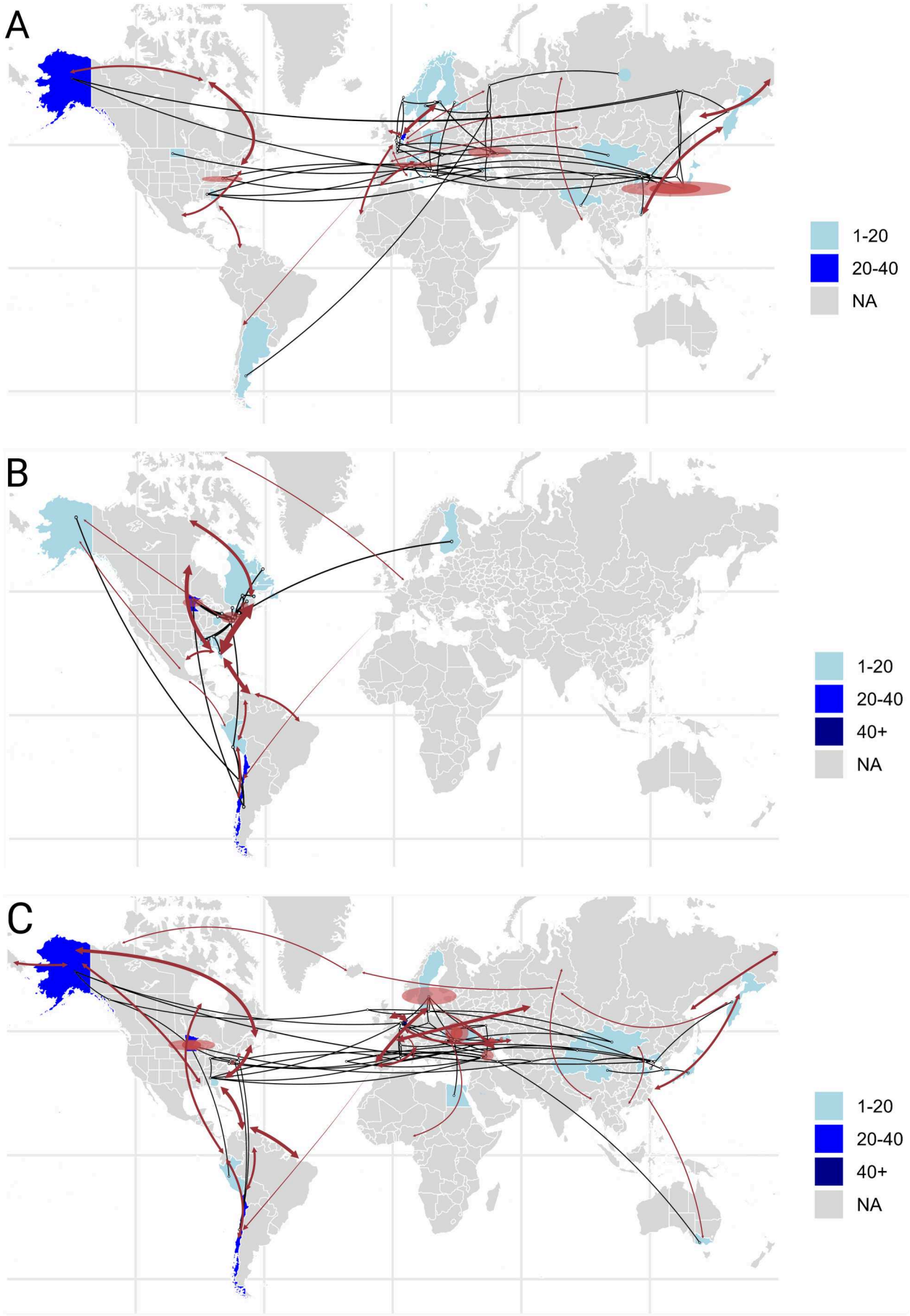

Figure 4. (A–G) Sequential illustration of the quantity, distribution, and geographic transmission patterns of H13 Groups A, B, and C and H16 Groups A, B, and C. The blue regions indicate virus quantities (Siberia, representing the vast region east of the Ural Mountains, is marked with a single blue circle for illustration). The black lines depict the geographic transmission routes of the viruses, whereas the dark red arrows represent the actual migration paths of the hosts. The arrow thickness corresponds to the number of host species involved. Viral diffusion curves that are concave upward indicate from east to west transmission. The red shaded area represents the 80% HPD interval. G The size of the blue circle represents the number of times involved in propagation.

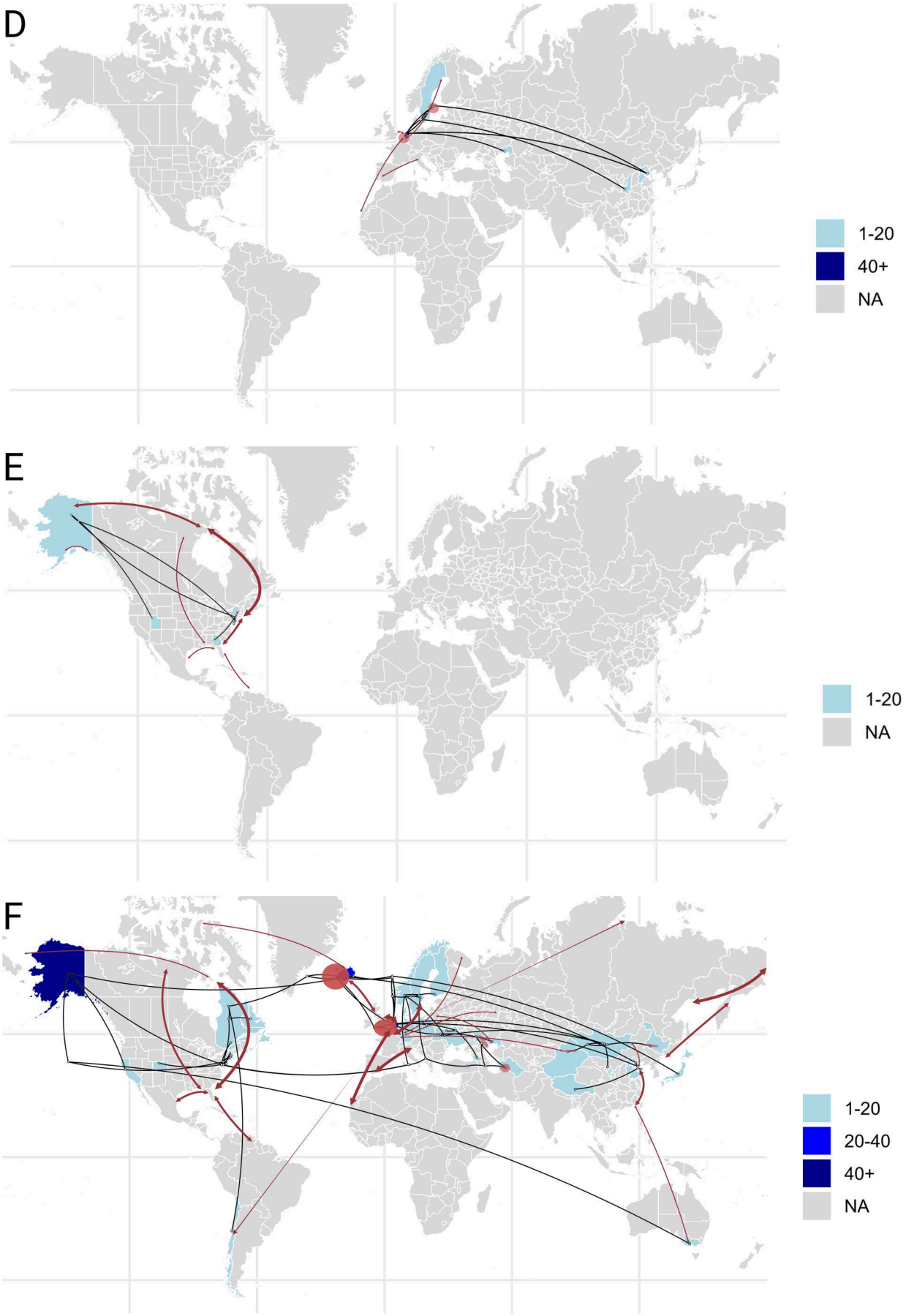

Figure 4. Continued.

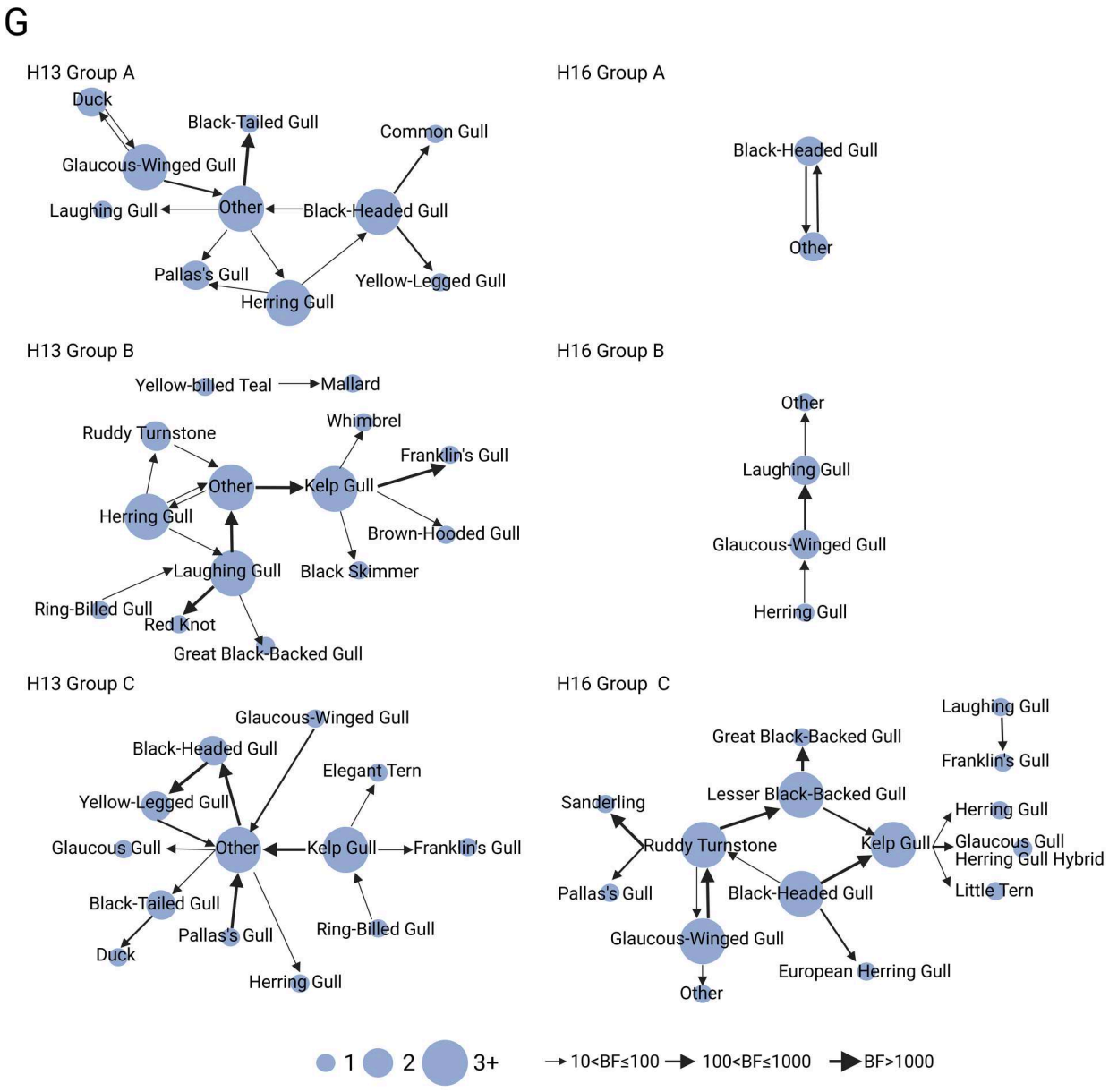

Figure 4. Continued.

skimmer, common snipe, Eurasian curlew, herring gull, mallard, Mediterranean gull, ring-billed gull, ruddy turnstone, semipalmated sandpiper, whimbrel, and yellow-legged gull. Phylogeographic analysis of H13 Group C hosts revealed that the major contributors to viral spread include the kelp gull, black-tailed gull, and yellow-legged gull (Figure 4(G), Table S5).

H16 AIVs

Continuous spatial diffusion analyzes of global H16 viruses were conducted based on the three branches identified by the HA gene MCC tree. Host information was analyzed using the discrete phylogenetic method. The characteristics of each branch are described below.

Group A is found in Europe (Sweden, the Netherlands, and Georgia) and China (Hebei and Shaanxi) (Figure 4(D)). Analysis of the geographical spread revealed that H16 Group A viruses are limited to Western Europe and China. The earliest known Group A virus was isolated in Atyrau, Kazakhstan, in 1983. The geographical spread of the viruses revealed that the virus initially spread locally from Sweden. Between 2005 and 2010, the spread expanded from Europe to central China. From 2010 to 2015, the virus spread from Europe to Bohai Bay in China and Central Asia. Between 2015 and 2020, the virus spread from the Netherlands back to Sweden. Migratory information was available for the black-headed gull and mallard. Phylogeographic analysis of H16 Group A hosts revealed that the black-headed gull was the major contributor to viral spread (Figure 4(G), Table S6).

Group B originates in the United States in North America (Figure 4(E)). The geographical spread analysis indicated that the H16 Group B viruses were

confined to North America. The earliest isolated Group B virus was traced back to Alaska, USA, in 1975. The geographical spread pathway revealed that the virus initially spread from Alaska to the East Coast of the United States. Between 2000 and 2005, the virus moved from the East Coast back to Alaska and the southern regions. From 2005 to 2010, the virus spread westward across the United States. Migratory information was available for the black-legged kittiwake, glaucous gull, herring gull, and red knot. Phylogeographic analysis of H16 Group B hosts revealed that the major contributors to viral spread include the laughing gull, glaucous-winged gull, and herring gull (Figure 4(G), Table S6).

Group C is distributed across Eurasia, the Americas, and Oceania (Figure 4(F)), with the greatest number of isolates found in Alaska in the USA and Iceland in Europe. In China, viruses are present in coastal and inland regions, including Xinjiang, Qinghai, Hebei, Shandong, and Liaoning. The viral spread routes involve five global migratory paths: the Pacific Americas, Mississippi Americas, Atlantic Americas, Central Asia, and East Asia–Australasia. Group C can be traced to viruses isolated in 1976 in Turkmenistan and Astrakhan, Russia. The geographical spread pathway indicates that this branch originated in Central Asia, initially spreading to nearby regions and reaching the East Coast of the United States and the northern continent in approximately 2000. Between 2000 and 2010, the virus continued to spread across various regions in Europe and expanded to Alaska in the USA, the eastern coast of Canada, Central Asia, and Mongolia. Iceland was a significant transmission hub during the spread from Europe to the Americas. From 2010–2015, the virus spread from Europe to Central Asia, Mongolia, and Japan; from Mongolia to Heilongjiang, China; from North America to South America; and from Alaska to the West Coast of the United States. Between 2015 and 2020, the virus spread from the East Coast of the United States to Alaska and Australia, from Iceland to inland Europe, from Europe to the surrounding regions, from the Bohai Bay area of China and Mongolia, and from Mongolia to Shaanxi, China. Migratory information was available for the black-headed gull, common gull, dunlin, glaucous gull, great black-backed gull, herring gull, red knot, mallard, northern pintail, ring-billed gull, ruddy turnstone, and sanderling. Phylogeographic analysis of H16 Group C hosts revealed that the major contributors to viral spread include the kelp gull, glaucous-winged gull, black-headed gull, and ruddy turnstone (Figure 4(G), Table S6).

H13 and H16 phylogenetic incongruence analyzes

Figure 5(A) shows that the reference viruses of H13 Groups A and C are distinctly scattered across the phylogenetic trees of other gene segments, exhibiting a wide distribution and significant potential for genetic exchange. These two branches include viruses originating from multiple continents. In contrast, Group B is more conserved and clustered within the phylogenetic trees of other gene segments. Except for one virus from Finland, all reference viruses originated from the Americas.

Figure 5(B) shows that the reference viruses of H16 Group C are distinctly scattered across the phylogenetic trees of other gene segments, exhibiting a broad distribution and significant potential for genetic exchange. This branch includes viruses from multiple continents. In contrast, Groups A and B are more conserved and clustered within the phylogenetic trees of other gene segments. The viruses in Group A mainly originated from four countries in Europe and Asia, whereas all the viruses in Group B originated exclusively from North America.

Genome analysis and genotypes

The nucleotide consensus alignment results of the H13, N2, N6, N8, PB2, PB1, PA, NP, M, and NS genes of the 28 H13 isolates were as follows: H13 gene: 75.2%−100%; N2 gene: 94.5%−100%; N6 gene: 95.0%−100%; N8 gene: 96.1%−99.1%; PB2 gene: 82.6%−100%; PB1 gene: 87.4%−100%; PA gene: 92.1%−100%; NP gene: 84.7%−100%; M gene: 91.6%−100%; and NS gene: 96.5%−100%. The nucleotide consensus alignment results of the H16, N2, N3, PB2, PB1, PA, NP, M, and NS genes of the 14 H16 isolates were as follows: H16: 79.5%−99.9%; N3: 91.8%−99.9%; PB2: 96.2%−100%; PB1: 95.1%−100%; PA: 91.4%−100%; NP: 84.8%−100%; M: 92.0%−100%; and NS: 86.5%−100%.

The HA protein cleavage site of the 28 H13 AIV strains was ISNR↓GLF or ISKR↓GLF (Table S7), and the site of the 14 H16 AIV strains was IN/VER↓GLF (Table S8), matching the characteristics of LPAIVs [43, 44]. Although the V186N and Q226L mutations, which are associated with enhanced binding affinity to the α-2,6 sialic acid receptor, were not absent in the HA proteins of the H13 and H16 viruses, the functionally analogous G228S mutation was identified [45–47]. Additionally, neither the 80–84 deletion in the NS1 protein [46] nor the E627K mutation in the PB2 protein, both of which are typically associated with enhanced virulence, were detected in the H13 and H16 viruses. However, several other mutations associated with enhanced viral lethality in mice and mammals were identified. These include the K389R and V598T mutations in the PB2 protein of the H13 isolates [48–50], the N66S mutation in the PB1-F2 protein of the XJ126 and XZ529 viruses, and the M105V and A184K mutations in the NP protein of the H13 isolates. Additionally, mutations in the

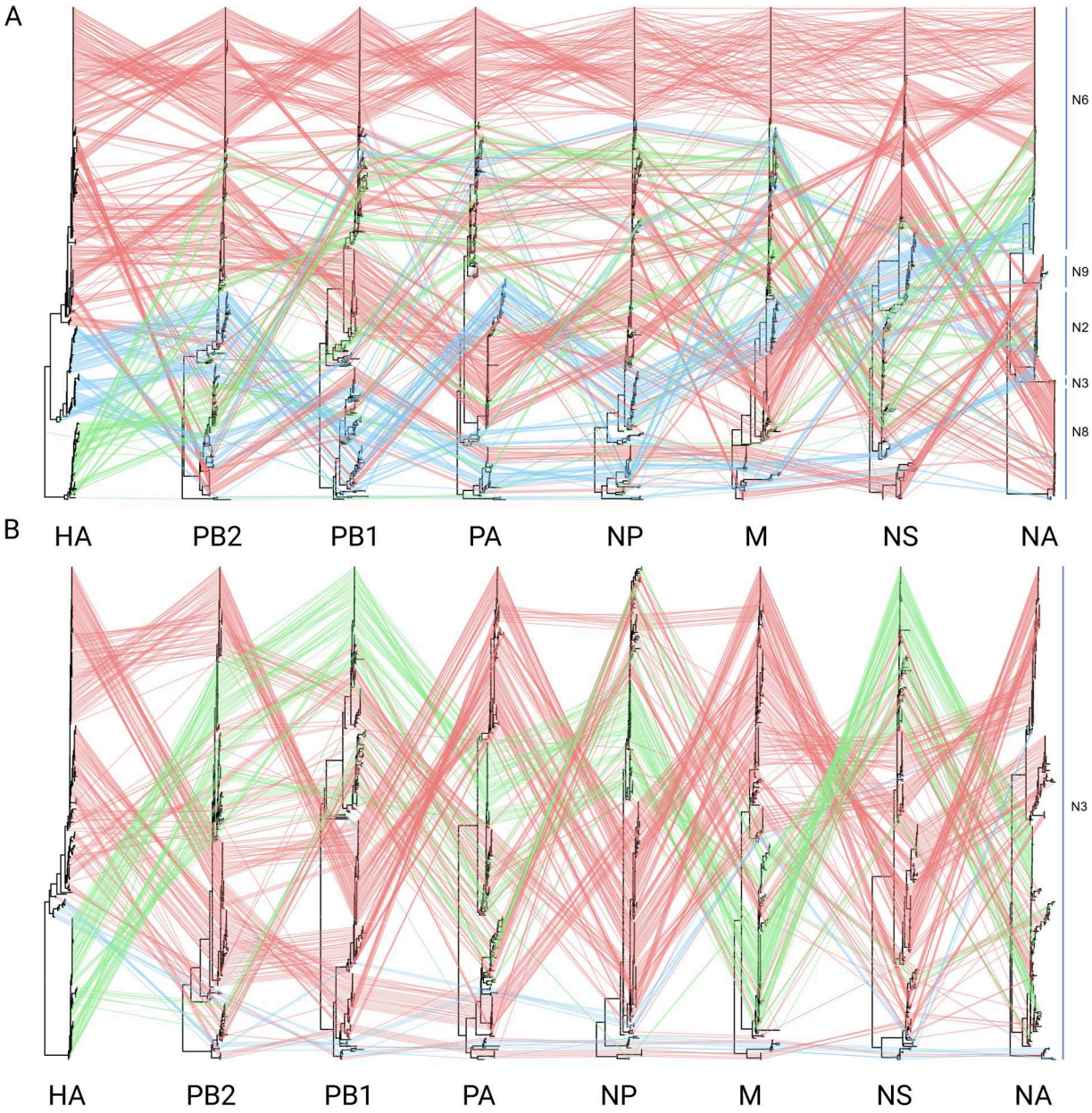

Figure 5. Phylogenetic incongruence analyses of H13 (A) and H16 (B) AIVs. Green, blue, and red colors indicate HA Groups A, B, and C, respectively.

M protein (N30D, I43M, and T215A) [51] were observed in both H13 and H16 isolates. Furthermore, mutations in the NS1 protein, including D74N, P42S, I106M, C138F, V149A, [L103F, I106M], and 227ESEV230, were also detected in the H13 and H16 isolates [52, 53]. Moreover, mutations such as S37A in the PA protein, which are linked to enhanced polymerase activity and replication efficiency in mammalian cell lines, were identified in both H13 and H16 isolates.

According to the differences in nucleotide consistency of the 6 internal genes (≤97% nucleotide consistency) and the topology of the evolutionary tree, the 28 H13 subtypes isolated in this study were classified into 17 genotypes (Table S9, Figure S1), and the 14 H16 viruses were classified into 9 genotypes (Table S10, Figure S2).

The H13 and H16 viruses analyzed in this study resulted primarily from frequent and complex genetic exchanges between Eurasian and North American lineages, and the viruses carried by wild waterfowl (especially gulls) during migration between Eurasia and North America may have exchanged gene fragments with the viruses carried by local poultry. The recombination of internal genes is far greater than that of external genes, the composition of genotypes is more complex, and the viral genetic diversity is high. The PB1 fragment of H13 G6/7/9 is clustered with the PA fragment of G2/5/8, and the PA fragment of H16 G3 is clustered with the N2 fragment of G4 and the domestic duck reference virus, indicating that these viruses may have recombined with viruses in poultry.

Replication and virulence of H13 and H16 viruses in mice

The replication of each representative virus in the mouse viscera at 72 h after infection with the H13 virus is shown in Figure 6(A). The black dotted lines indicate the lowest value at which the virus was not detected in the viscera. According to the virus titration results, replication of the H13 subtype virus in mice is not significantly effective, as indicated by low titres, and is dominated by digestive tract replication. In the digestive system, the virus titre was 0.58–0.83 $\log_{10}$ EID_{50} in the mouse rectum, whereas the titres in the other organs were 0.58 $\log_{10}$ EID_{50}, except G13/15, which had greater replication efficiency than the other viruses did. The virus replication titre in the nasal turbinate and lung in the respiratory system was 0.58 $\log_{10}$ EID_{50}. The replication of each representative virus in the mouse viscera at 72 h after infection with the H16 subtype virus is shown in Figure 6(B). According to the virus titration results, all genotypes of H16 viruses other than G5 can infect mice and have different replication effects in different tissues, mainly the respiratory system. In the respiratory system, lung infection dominated, where G2/9 had good replication in mouse lungs. The average titres of the viruses in the mouse lung and turbinate were 0.83–3 $\log_{10}$ EID_{50} and 0.58 $\log_{10}$ EID_{50}, respectively. In the digestive system, the virus replicated at low levels in the kidney, spleen, and rectum, with an average titre of 0.58–0.83 $\log_{10}$ EID_{50}.

Changes in the weights of H13 and H16 subtype virus-infected mice after 14 days are shown in Figure 6(C,D). The virus is not fatal to mice, with a survival rate of 100%, and there are no obvious clinical symptoms. Within 14 days, the body weight fluctuated slightly, and the overall body weight tended to increase normally.

Discussion

From 20 years of data from avian influenza surveillance in wild birds in China, we isolated 47 H13 and H16 subtypes of AIVs. The HA phylogenetic trees were divided into three distinct clades. H13 viruses in Groups A and C are distributed across multiple global regions, whereas Group B viruses are restricted to North and South America. Most hosts of H13 viruses are *Charadriiformes*, with a small number belonging to *Anseriformes*, turkeys, and whales. The viruses in this study are distributed primarily in Groups A and C. In contrast, the H13N2 virus isolated from a pilot whale in 1984 is located in Group B, with a nucleotide sequence divergence of 79.1%–81.4% compared with that of the viruses isolated by our laboratory. Bayesian analysis indicates that North America and Europe are the central regions for H13 dissemination. The

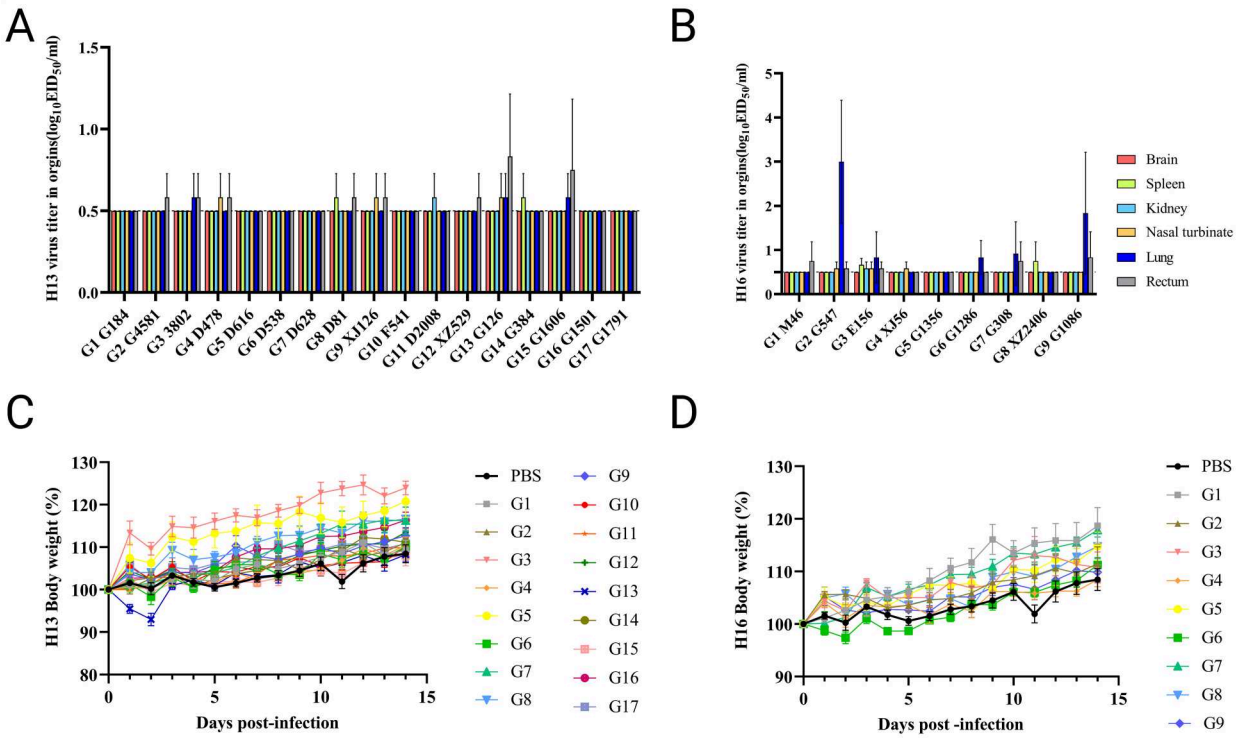

Figure 6. Replication of H13 (A) and H16 (B) viruses in mice. Viral titers in the organs of the mice that were euthanized at 3 d post-inoculation with 10^6 EID_{50} of each test virus. The dashed lines indicate the lower limit of virus detection. The color bar shows the mean of three replicates; the error bar indicates the standard deviation. Virulence of H13 (C) and H16 (D) viruses in mice. Body weight changes of the mice after inoculation with 10^6 EID_{50} of each test virus. Each dot represents the average body weight of 5 mice.

evidence suggests that the virus spreads bidirectionally between North America and South America, as well as between North America and Europe. However, only unidirectional spread is observed from Europe to East Asia, which contrasts with the spread of highly pathogenic H5 viruses from Asia to Europe. This result is consistent with existing study findings [13]. Group A H16 viruses are distributed globally, Group B viruses are limited to North America and a few European regions, and Group C viruses are found only in China and a few European regions. Most hosts of H16 viruses belong to the *Charadriiformes* order, with a small number of hosts from *Anseriformes* and other species. The viruses in this study are primarily distributed in Groups A and C. Bayesian analysis revealed that Europe is the central region for H16 dissemination, with spread occurring from Europe to the Americas and East Asia. With respect to hosts, studies have shown that long-distance gull migration facilitates the intercontinental genetic exchange of AIVs between Eurasia and the Americas. Gulls are considered genetic mixers of different lineages of avian influenza, similar to the role of pigs in human influenza [16, 17, 19, 54]. Bayesian host analysis for H13 viruses identified the black-headed gull, kelp gull, laughing gull, ruddy turnstone, and herring gull as key hosts for viral dissemination. Bayesian host analysis for H16 viruses identified the black-headed gull, herring gull, laughing gull, and glaucous-winged gull as key hosts for viral dissemination. Most hosts are long-distance migratory animals, which likely facilitates the transmission of the virus between habitats with the migration paths acting as bridges for viral spread and gene flow on a global scale. H13 Groups A and C and H16 Group C are widely distributed, whereas the other groups are more limited and isolated. Therefore, we conducted independent analyzes of the HA segments of the three groups for both H13 and H16 viruses and constructed eight-segment phylogenetic tangles to explore the underlying mechanism.

Through the analysis of continuous virus transmission within each group, we determined that H13 Groups A and C and H16 Group C presented evidence of gene exchange across multiple continents, including the Americas and Europe, Europe and Central Asia, and Central Asia and the Americas. Furthermore, H13 Group A demonstrated gene exchange between East Asia and Alaska (United States), as well as between East Asia and Europe. In contrast, H16 Groups A and B showed no intercontinental exchange, whereas H13 Group B exhibited genetic exchange only between North and South America. This finding highlights the cyclic transmission patterns of viral genes among different groups. Widely distributed groups often exhibit intercontinental genetic exchange and clear viral transmission chains, which may be closely linked to the migratory behaviour of host species. To test this hypothesis, we collected host information from migratory satellite data and observed significant spatial overlap between host migration routes and viral dissemination patterns. Globally distributed groups tended to have broader migratory ranges, with a notable concentration in Europe. This finding may be biased by tracker deployment locations; however, viral dissemination data indicate that Europe remains a key hub for intercontinental viral transmission. In contrast, hosts of independent groups in the Americas exhibit migration patterns concentrated within the Americas. This finding supports the view that viral transmission within the Americas is relatively isolated and lacks intercontinental genetic exchange. These migratory patterns may create a relatively closed transmission network, restricting the intercontinental spread of these viruses. Additionally, phylogenetic incongruence analyzes of the complete gene segments of the H13 and H16 subtypes revealed extensive potential reassortment among global viruses. The reference viruses of H13 Groups A and C and H16 Group C are scattered across three branches of other gene segments, indicating extensive genetic exchange. In contrast, other geographically restricted groups are more conserved, with limited scattering in tanglegrams. These findings suggest that the formation of independent lineages of H13 and H16 subtypes may be closely related to intercontinental genetic exchange and the migratory behaviour of their hosts. We recommend increased international collaboration and expanded tracker deployment locations to better understand the relationships between viruses and migratory hosts.

Additionally, we analyzed the distributions of all the hosts. Our analysis revealed that 9 out of 21 hosts of H13 Group B viruses were distributed in the Americas, which was a significantly greater proportion than the hosts of Group A (4/22) and Group C (12/29) viruses. This difference suggests that host activity regions may limit virus transmission by creating geographical isolation, leading to reduced genetic exchange between viral groups and the independent evolution of Group B viruses. Interestingly, some Group B hosts have a global distribution but have not facilitated widespread global transmission of Group B viruses. This event may be attributed to habitat differences among host subspecies. Even widely distributed hosts may have limited activity ranges and non-overlapping habitats, resulting in geographical isolation. In contrast, viruses in Group A and Group C can infect globally distributed hosts, likely due to a more significant overlap between host migration routes and habitats, which facilitates wider viral dissemination. On the basis of this theory, we recommend focusing on host habitat characteristics and activity range distributions in viral transmission

studies, with particular attention given to migration routes and habitat overlap. These factors likely play a significant role in viral spread and evolution. Therefore, we propose targeted sampling in overlapping migration areas of migratory birds and the use of satellite tracking to monitor the migration routes of globally distributed hosts to assess their potential for virus transmission. Specifically, H13-associated globally distributed hosts include the black-headed gull, black-legged kittiwake, common murre, dunlin, Eurasian curlew, glaucous gull, little gull, red knot, ruddy turnstone, sanderling, and whimbrel. For H16, the hosts include the black-headed gull, common gull, dunlin, Eurasian coot, lesser black-backed gull, little tern, northern pintail, red knot, and ruddy turnstone. Among these globally distributed species, particular attention should be given to transcontinental hosts whose migrations may facilitate viral spread between continents. For example, glaucous-winged gulls, dunlins, and glaucous gulls in the Bering Strait may promote virus transmission between Alaska and Northeast Asia, resembling the spread of H5N8 HPAIV from East Asia to North America via the Bering Strait [55]. Iceland gulls migrate between northern Europe and North America, potentially accelerating viral transmission between the two continents. Analyzing host activity patterns and habitat overlaps can increase our understanding of viral transmission pathways and inform future monitoring and control strategies.

Unlike previous studies, this study examined the infectivity and pathogenicity of H13 and H16 viruses in mice and demonstrated that these two viruses can infect mice without prior adaptation and exhibit low pathogenicity [56, 57]. The possible reason might be the amino acid substitutions in the H13 and H16 viruses, which were not included among the mutations reported in previous studies. Alternatively, H16 may have undergone genetic reassortment with other viruses. Among the representative viruses, 10 H13 viruses and 8 H16 viruses presented low-level replication in mouse organs. Some representative viruses of the H13 subtype, including G184, D161, D538, D628, F541, G1501, and G1791, failed to replicate effectively in mice. Among these viruses, G184, F541, and D616 presented no evidence of internal gene reassortment with HPAIV gene segments. The PB2 protein of G150 exhibited an L339T mutation, which has been associated with reduced pathogenicity in mice. Neither D538 nor D628 presented the I292V mutation in the PB2 protein, a site known to increase the pathogenicity of the virus in mice and other mammals. Among the H16 viruses, G1356 failed to replicate in mice. The mechanisms influencing the infection and replication of the virus in mice are complex, and further research is needed to elucidate the details.

The results revealed that H13 and H16 AIVs did not cause weight loss in mice, but most of the genotypes (H13 10/17; H16 8/9) replicated in mice, indicating a risk of the virus infecting mammals across interspecific barriers and a threat to public health. Gulls are the natural hosts of H13 and H16 viruses, and their long-distance migration facilitates recombination between Eurasian and North American lineage viruses. Owing to the segmented nature of the AIV genome, H13 and H16 AIVs have incorporated gene fragments from poultry-derived viruses, increasing their genetic diversity. This increased diversity may lead to broader or prolonged viral spread, posing potential risks to poultry and mammals in the future [58–60].

Acknowledgements

We thank the authors and submitting laboratories of the sequences from the Global Initiative on Sharing All Influenza Data (GISAID, https://www.gisaid.org) EpiFlu database. We thank the authors and submitting labs of the data from the MoveBank (https://www.movebank.org) database. We thank American Journal Experts LLC (https://www.aje.cn/) for editing this manuscript.

Disclosure statement

No potential conflict of interest was reported by the author(s).

Funding

This work was supported by the National Key Research and Development Program of the National Forestry and Grassland Administration, Biological Disaster Prevention and Control Center [grant number 2022YFC2303801], the Fundamental Research Funds for the Central Universities, China [grant number 2572022CG01], the China Postdoctoral Science Foundation [grant number 2024M760389 and GZC20230401], Heilongjiang Postdoctoral Fund [grant number LBH-Z24045], Major Project of Guangzhou National Laboratory [grant number GZNL2023A01001], and the National Forestry and Grassland Administration, China.

ORCID

Xiang Li1 http://orcid.org/0009-0000-9613-1512
Xiang Li2 http://orcid.org/0000-0003-2879-3957
Hongliang Chai http://orcid.org/0000-0001-7162-2497

References

[1] Wu Y, Wu Y, Tefsen B, et al. Bat-derived influenza-like viruses H17N10 and H18N11. Trends Microbiol. 2014 Apr;22(4):183–191. doi:10.1016/j.tim.2014.01.010

[2] Fereidouni S, Starick E, Karamendin K, et al. Genetic characterization of a new candidate hemagglutinin subtype of influenza A viruses. Emerg Microbes

Infect. 2023 Dec;12(2):2225645. doi:10.1080/22221751.2023.2225645
[3] Yoon SW, Webby RJ, Webster RG. Evolution and ecology of influenza A viruses. Curr Top Microbiol Immunol. 2014;385:359–375. doi:10.1007/82_2014_396
[4] Wille M, Holmes EC. The ecology and evolution of influenza viruses. Cold Spring Harb Perspect Med. 2020 Jul;10(7):a038489. doi:10.1101/cshperspect.a038489
[5] Yu Z, Cheng K, Gao Y. Poultry infection with influenza viruses of wild bird origin, China, 2016. Emerg Infect Dis. 2018 Jul;24(7):1375–1377. doi:10.3201/eid2407.171220
[6] Lupiani B, Reddy SM. The history of avian influenza. Comp Immunol Microbiol Infect Dis. 2009 Jul;32(4):311–23. doi:10.1016/j.cimid.2008.01.004
[7] Hinshaw VS, Air GM, Gibbs AJ, et al. Antigenic and genetic characterization of a novel hemagglutinin subtype of influenza A viruses from gulls. J Virol. 1982 Jun;42(3):865–872. doi:10.1128/JVI.42.3.865-872.1982
[8] Yu Z, He H, Cheng K, et al. Genetic characterization of an H13N2 low pathogenic avian influenza virus isolated from gulls in China. Transbound Emerg Dis. 2019 Mar;66(2):1063–1066. doi:10.1111/tbed.13108
[9] Dong J, Bo H, Zhang Y, et al. Characteristics of influenza H13N8 subtype virus firstly isolated from Qinghai Lake Region, China. Virol J. 2017;14(1):180. doi:10.1186/s12985-017-0842-1
[10] Wang Y, Zhang H, Wang M, et al. Genetic analysis of a novel H16N3 virus isolated from a migratory gull in China in 2021 and animal studies of infection. Microbiol Spectr. 2022 Dec;10(6):e0248422. doi:10.1128/spectrum.02484-22
[11] Li Y, Li M, Tian J, et al. Characteristics of the first H16N3 subtype influenza A viruses isolated in western China. Transbound Emerg Dis. 2020 Jul;67(4):1677–1687. doi:10.1111/tbed.13511
[12] Peng P, Shen J, Shi W, et al. Novel H16N3 avian influenza viruses isolated from migratory gulls in China in 2023. Front Microbiol. 2025 Jan;15:1543338. doi:10.3389/fmicb.2024.1543338
[13] Verhagen JH, Poen M, Stallknecht DE, et al. Phylogeography and antigenic diversity of low-pathogenic avian influenza H13 and H16 viruses. J Virol. 2020 Jun;94(13):e00537-20. doi:10.1128/JVI.00537-20
[14] Sun W, Zhao M, Yu Z, et al. Cross-species infection potential of avian influenza H13 viruses isolated from wild aquatic birds to poultry and mammals. Emerg Microbes Infect. 2023 Dec;12(1):e2184177. doi:10.1080/22221751.2023.2184177
[15] Wille M, Robertson GJ, Whitney H, et al. Reassortment of American and Eurasian genes in an influenza A virus isolated from a great black-backed gull (Larus marinus), a species demonstrated to move between these regions. Arch Virol. 2011 Jan;156(1):107–115. doi:10.1007/s00705-010-0839-1
[16] Li Y, Li X, Lv X, et al. Highly pathogenic avian influenza A (H5Nx) virus of clade 2.3.4.4b emerging in Tibet, China, 2021. Microbiol Spectr. 2022;10(3):e00643-22. doi:10.1128/spectrum.00643-22
[17] Ratanakorn P, Wiratsudakul A, Wiriyarat W, et al. Satellite tracking on the flyways of brown-headed gulls and their potential role in the spread of highly pathogenic avian influenza H5N1 virus. PLoS One. 2012;7(11):e49939. doi:10.1371/journal.pone.0049939
[18] Wille M, Robertson GJ, Whitney H, et al. Extensive geographic mosaicism in avian influenza viruses from gulls in the northern hemisphere. PLoS One. 2011;6(6):e20664. doi:10.1371/journal.pone.0020664
[19] Li X, Lv X, Li Y, et al. Highly pathogenic avian influenza A(H5N8) virus in Swans, China, 2020. Emerg Infect Dis. 2021 Jun;27(6):1732–1734. doi:10.3201/eid2706.204727
[20] Van Borm S, Rosseel T, Vangeluwe D, et al. Phylogeographic analysis of avian influenza viruses isolated from Charadriiformes in Belgium confirms intercontinental reassortment in gulls. Arch Virol. 2012 Aug;157(8):1509–1522. doi:10.1007/s00705-012-1323-x
[21] Li X, Lv X, Li Y, et al. Emergence, prevalence, and evolution of H5N8 avian influenza viruses in central China, 2020. Emerg Microbes Infect. 2022 Dec;11(1):73–82. doi:10.1080/22221751.2021.2011622
[22] Cui Y, Li Y, Li M, et al. Evolution and extensive reassortment of H5 influenza viruses isolated from wild birds in China over the past decade. Emerg Microbes Infect. 2020 Dec;9(1):1793–1803. doi:10.1080/22221751.2020.1797542
[23] Cheung PP, Leung YH, Chow CK, et al. Identifying the species-origin of faecal droppings used for avian influenza virus surveillance in wild-birds. J Clin Virol. 2009 Sep;46(1):90–93. doi:10.1016/j.jcv.2009.06.016
[24] Lv X, Tian J, Li X, et al. H10Nx avian influenza viruses detected in wild birds in China pose potential threat to mammals. One Health. 2023 Feb;16:100515. doi:10.1016/j.onehlt.2023.100515
[25] Buyanravjikh S, Han S, Lee S, et al. [Corrigendum] Cryptotanshinone inhibits IgE-mediated degranulation through inhibition of spleen tyrosine kinase and tyrosine–protein kinase phosphorylation in mast cells. Mol Med Rep. 2021 Sep;24(3):644. doi:10.3892/mmr.2021.12283
[26] Tavares ES, Baker AJ. Single mitochondrial gene barcodes reliably identify sister-species in diverse clades of birds. BMC Evol Biol. 2008 Mar;8:81. doi:10.1186/1471-2148-8-81
[27] Lee DH, Lee HJ, Lee YN, et al. Application of DNA barcoding technique in avian influenza virus surveillance of wild bird habitats in Korea and Mongolia. Avian Dis. 2010 Mar;54(Suppl 1):677–681. doi:10.1637/8783-040109-ResNote.1
[28] Katoh K, Standley DM. MAFFT multiple sequence alignment software version 7: improvements in performance and usability. Mol Biol Evol. 2013 Apr;30(4):772–780. doi:10.1093/molbev/mst010
[29] Zhang D, Gao F, Jakovlić I, et al. Phylosuite: An integrated and scalable desktop platform for streamlined molecular sequence data management and evolutionary phylogenetics studies. Mol Ecol Resour. 2020 Jan;20(1):348–355. doi:10.1111/1755-0998.13096
[30] Kalyaanamoorthy S, Minh BQ, Wong TKF, et al. Modelfinder: fast model selection for accurate phylogenetic estimates. Nat Methods. 2017 Jun;14(6):587–589. doi:10.1038/nmeth.4285
[31] Drummond AJ, Rambaut A. BEAST: Bayesian evolutionary analysis by sampling trees. BMC Evol Biol. 2007 Nov;7:214. doi:10.1186/1471-2148-7-214
[32] Drummond AJ, Ho SY, Phillips MJ, et al. Relaxed phylogenetics and dating with confidence. PLoS Biol. 2006 May;4(5):e88. doi:10.1371/journal.pbio.0040088

[33] Suchard MA, Lemey P, Baele G, et al. Bayesian phylogenetic and phylodynamic data integration using BEAST 1.10. Virus Evol. 2018 Jun;4(1):vey016. doi:10.1093/ve/vey016
[34] Chai H, Li X, Li M, et al. Emergence, evolution, and pathogenicity of influenza A(H7N4) virus in shorebirds in China. J Virol. 2022 Feb;96(3):e0171721. doi:10.1128/JVI.01717-21
[35] Baele G, Lemey P, Bedford T, et al. Improving the accuracy of demographic and molecular clock model comparison while accommodating phylogenetic uncertainty. Mol Biol Evol. 2012 Sep;29(9):2157–2167. doi:10.1093/molbev/mss084
[36] Rambaut A, Drummond AJ, Xie D, et al. Posterior summarization in Bayesian phylogenetics using tracer 1.7. Syst Biol. 2018 Sep;67(5):901–904. doi:10.1093/sysbio/syy032
[37] Bielejec F, Baele G, Vrancken B, et al. Spread3: interactive visualization of spatiotemporal history and trait evolutionary processes. Mol Biol Evol. 2016 Aug;33(8):2167–2169. doi:10.1093/molbev/msw082
[38] Kays R, Davidson SC, Berger M, et al. The Movebank system for studying global animal movement and demography. Methods in Ecology and Evolution. 2021;13(2):419–431. doi:10.1111/2041-210X.13767
[39] Villanueva RAM, Chen ZJ. Ggplot2: elegant graphics for data analysis (2nd ed.). Measurement: Interdisciplinary Research and Perspectives. 2019;17(3):160–167. doi:10.1080/15366367.2019.1565254
[40] Wickham H, François R, Henry L, et al. dplyr: A Grammar of Data Manipulation. R Package Version 1.1.4, 2023. Available from: https://github.com/tidyverse/dplyr, https://dplyr.tidyverse.org
[41] Yu G. Using ggtree to visualize data on tree-like structures. Current Protocols in Bioinformatics. 2020;69:e96. doi:10.1002/cpbi.96
[42] Paradis E, Schliep K. Ape 5.0: an environment for modern phylogenetics and evolutionary analyses in R. Bioinformatics. 2019;35:526–528. doi:10.1093/bioinformatics/bty633
[43] Chen H, Yuan H, Gao R, et al. Clinical and epidemiological characteristics of a fatal case of avian influenza A H10N8 virus infection: a descriptive study. Lancet. 2014 Feb;383(9918):714–721. doi:10.1016/S0140-6736(14)60111-2
[44] Schneider EK, Li J, Velkov T. A portrait of the sialyl glycan receptor specificity of the H10 influenza virus hemagglutinin: a picture of an avian virus on the verge of becoming a pandemic? Vaccines (Basel). 2017 Dec;5(4):51. doi:10.3390/vaccines5040051
[45] Lu X, Qi J, Shi Y, et al. Structure and receptor binding specificity of hemagglutinin H13 from avian influenza A virus H13N6. J Virol. 2013 Aug;87(16):9077–9085. doi:10.1128/JVI.00235-13
[46] Suttie A, Deng YM, Greenhill AR, et al. Inventory of molecular markers affecting biological characteristics of avian influenza A viruses. Virus Genes. 2019 Dec;55(6):739–768. doi:10.1007/s11262-019-01700-z
[47] Gao XL, Fan ST, Li SN, et al. Phylogenetic analysis and assessment of the pathogenicity and transmissibility of the H13N6 subtype AIV firstly isolated from China. Chin J Prev Vet Mede. 2015;37(3):172–176. doi:10.3969/j.issn.1008-0589.2015.03.03
[48] Gao W, Zu Z, Liu J, et al. Prevailing I292V PB2 mutation in avian influenza H9N2 virus increases viral polymerase function and attenuates IFN-β induction in human cells. J Gen Virol. 2019 Sep;100(9):1273–1281. doi:10.1099/jgv.0.001294
[49] Subbarao EK, London W, Murphy BR. A single amino acid in the PB2 gene of influenza A virus is a determinant of host range. J Virol. 1993 Apr;67(4):1761–1764. doi:10.1128/JVI.67.4.1761-1764.1993
[50] Li Z, Chen H, Jiao P, et al. Molecular basis of replication of duck H5N1 influenza viruses in a mammalian mouse model. J Virol. 2005 Sep;79(18):12058–12064. doi:10.1128/JVI.79.18.12058-12064.2005
[51] Nao N, Kajihara M, Manzoor R, et al. A single amino acid in the M1 protein responsible for the different pathogenic potentials of H5N1 highly pathogenic avian influenza virus strains. PLoS One. 2015 Sep;10(9):e0137989. doi:10.1371/journal.pone.0137989
[52] Jiao P, Tian G, Li Y, et al. A single-amino-acid substitution in the NS1 protein changes the pathogenicity of H5N1 avian influenza viruses in mice. J Virol. 2008 Feb;82(3):1146–1154. doi:10.1128/JVI.01698-07
[53] Kuo RL, Krug RM. Influenza a virus polymerase is an integral component of the CPSF30-NS1A protein complex in infected cells. J Virol. 2009 Feb;83(4):1611–1616. doi:10.1128/JVI.01491-08
[54] Ineson KM, Hill NJ, Clark DE, et al. Age and season predict influenza A virus dynamics in urban gulls: consequences for natural hosts in unnatural landscapes. Ecol Appl. 2022 Mar;32(2):e2497. doi:10.1002/eap.2497
[55] Lee DH, Torchetti MK, Winker K, et al. Intercontinental spread of Asian-origin H5N8 to North America through Beringia by migratory birds. J Virol. 2015 Jun;89(12):6521–6524. doi:10.1128/JVI.00728-15
[56] Sun LY, Li YG, Zhang XH, et al. A genetic evolutionary analysis and an evaluation of the infectivity of avian influenza H16N3 isolated from wild birds in China. J Pathog Biol. 2020;15(12):1370–1376. doi:10.13350/j.cjpb.201202
[57] Caliendo V, Kleyheeg E, Beerens N, et al. Effect of 2020–21 and 2021–22 highly pathogenic avian influenza H5 epidemics on wild birds, The Netherlands. Emerg Infect Dis. 2024 Jan;30(1):50–57. doi:10.3201/eid3001.230970
[58] USDA APHIS. 2022–2024 detections of highly pathogenic avian influenza in wild birds, 2024. Available from. https://www.aphis.usda.gov/aphis/ourfocus/animalhealth/animal-disease-information/avian/avian-influenza/hpai-2022/2022-hpai-wild-birds
[59] Hill NJ, Bishop MA, Trovão NS, et al. Ecological divergence of wild birds drives avian influenza spillover and global spread. PLoS Pathog. 2022 May;18(5):e1010062. doi:10.1371/journal.ppat.1010062
[60] Fan S, Deng G, Song J, et al. Two amino acid residues in the matrix protein M1 contribute to the virulence difference of H5N1 avian influenza viruses in mice. Virology. 2009 Feb;384(1):28–32. doi:10.1016/j.virol.2008.11.044